

The Study of Dynamic Slug Flow Characteristics Using Digital Image Analysis—Part I: Flow Visualization

M. Gopal

e-mail: mgopal@bobcat.ent.ohiou.edu

W. P. Jepson

e-mail: jepson@bobcat.ent.ohiou.edu

NSF, I/UCRC Corrosion in
Multiphase Systems Center,
Department of Chemical Engineering,
Ohio University,
Athens, OH 45701

This paper reports the application of novel, digital image analysis techniques in the study of slug flow characteristics, under dynamic conditions in two-phase gas-liquid mixtures. Water and an oil of viscosity 18 cP were used for the liquid phase and carbon dioxide was used for the gas phase. Flow in a 75-mm i.d., 10-m long acrylic pipeline system was studied. Images of slugs were recorded on video by S-VHS cameras, using an audio-visual mixer. Each image was then digitized frame-by-frame and analyzed on a SGI™ workstation. Detailed slug characteristics, including liquid film heights, slug translational velocity, mixing length, and, slug length, were obtained.

Introduction

Multiphase transportation in long-distance flow lines has become a key technological feature in oil and gas production. The accurate prediction of multiphase flow characteristics in the flow lines is essential for their safe design and economical operation. Various flow regimes are seen in multiphase flow. These include stratified, plug, slug, and annular flow regimes. The production rates in oil and gas wells are such that, in most cases, the multiphase flow lines are normally in slug flow. Slugs are highly turbulent and can lead to increased pipe damage from internal corrosion and mechanical impacts.

Figure 1 shows the profile of a slug. Waves form on the liquid film, that grow to bridge the pipe, causing the liquid to be accelerated by the gas. As the slug front moves through the pipe, it overruns slow-moving liquid film ahead of it and accelerates it to the velocity of the slug. A mixing vortex is created in this process. This leads to a scouring mechanism on the pipe wall with high rates of shear. Also, as the liquid is scooped up into the slug, the leading edge of the slug jumps to the top of the pipe, entraining considerable amounts of gas in its wake. This leads to the creation of a highly frothy turbulent region behind the slug front called the mixing zone. The liquid and gas are assimilated into the slug and accelerated to the velocity of the slug in this region of the slug. The gas is released in the mixing zone in the form of pulses of bubbles (Jepson, 1987). These bubbles are trapped by the mixing vortex and forced towards the bottom of the pipe, where they can impact and can collapse. The high rates of shear due to the mixing vortex and the bubble impact and collapse can significantly increase corrosion of the pipe wall.

Beyond the mixing region of the slug, the level of turbulence is reduced, and buoyancy forces move the gas towards the top of the pipe. The cross-sectional area available for liquid flow increases and the liquid velocity decreases. This is the slug body. Eventually, a point is reached where the liquid velocity is no longer sufficient to sustain the bridging of the pipe, and the liquid level falls off. This is called the slug tail. The liquid velocity decreases in the liquid film, its height rebuilds, with waves forming on its surface and the next slug is initiated.

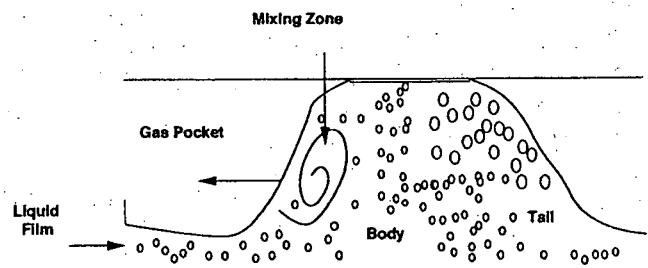


Fig. 1 Profile of a slug

Slug characteristics have been measured by several researchers. Nicholson et al. (1978) measured slug characteristics and extended the model by Dukler and Hubbard (1975). Kouba (1984) carried out a detailed investigation of horizontal slug flow characteristics and measured slug velocities, holdup, and liquid film heights. In this paper, a novel visualization technique is described that is used to measure local, instantaneous slug characteristics, such as slug translational velocity and liquid film heights between slugs. In addition, velocity and void fraction profiles in the mixing zone, slug body, and slug tail were also measured. Those results have been published elsewhere (Gopal and Jepson, 1997). In Part II of this study (Gopal and Jepson, 1998), the results are used in constructing a mathematical model for the prediction of slug characteristics.

Flow visualization has been used extensively in many different applications over the years, and several techniques are currently in existence (Miles and Lempert, 1997). Of the most popular techniques are LDA/LDV (laser doppler anemometry/velocimetry), PIV (particle image velocimetry), and nuclear radiation techniques. PIV is used with the assumption of no local slip between the particles (bubbles) and the continuous phase. Luo et al. (1997) describe a direct flow visualization technique that was used to study the hydrodynamics and heat transfer characteristics of high-pressure fluidized bed reactors and proposed mechanisms involving bubble coalescence and breakup. The mixing zone of slugs has been studied using flow visualization (Gopal et al., 1995) and unique gas/liquid mixing mechanisms and their effect of corrosion of pipe walls have been described.

Experimental Procedure

Figure 2 shows a schematic view of the experimental setup. Liquid is stored in a 0.6-m³ stainless steel tank and is pumped

Contributed by the Petroleum Division for publication in the JOURNAL OF ENERGY RESOURCES TECHNOLOGY. Manuscript received by the Petroleum Division, December 5, 1996; revised manuscript received January 19, 1998. Technical Editor: J. P. Brill.

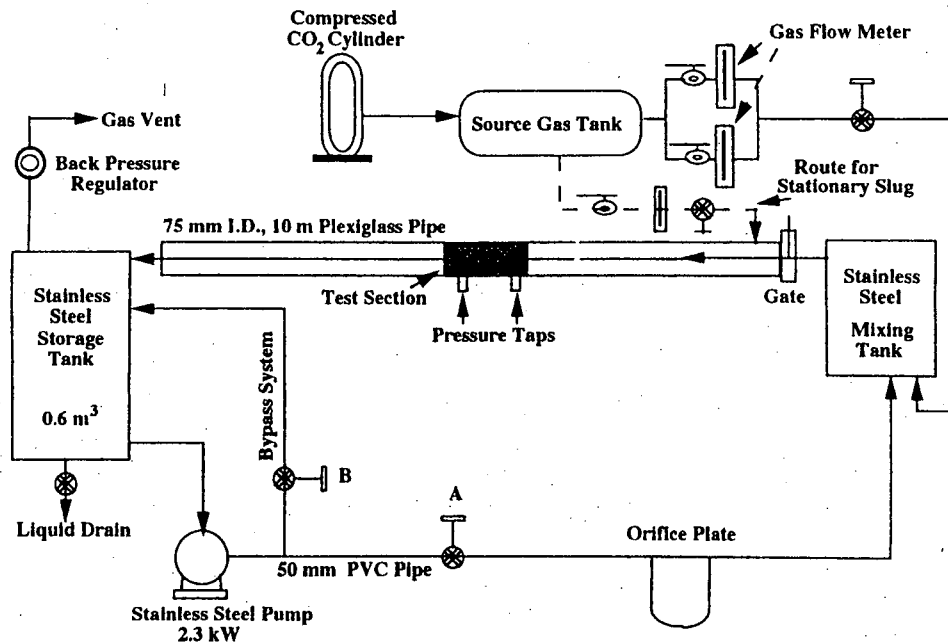


Fig. 2 Schematic diagram of experimental system

Table 1 Experimental test matrix^(a)

Variable	Deionised Water	ARCOPAK90	Carbon dioxide
Density (kg/m ³)	998	850	1.9
Viscosity (Pa.s)	0.0010	0.015	0.000015
Surface Tension in air (N/m)	0.070	0.040	-
Superficial Velocity (m/s)	0.2 - 1.3	0.16 - 0.88	1 - 5

^(a) The range of velocities cover the entire range of the slug flow regime; all values are listed for 298 K and 101.3 kPa

by a 2.3-kW stainless steel centrifugal pump into a 50-mm i.d. PVC pipe. The flow rate of the liquid is controlled by a bypass system and is monitored by an orifice plate. Carbon dioxide from compressed cylinders is stored in a 1.67-m³ carbon dioxide tank at a pressure of 1300 kPa. It is introduced into the system at an inlet pressure of 800 kPa. The gas flow rate is controlled by a flow regulating valve and is monitored by variable area gas flow meters. Slugs are generated and the two-phase mixture is allowed to flow out into the 7.5-cm-dia, 10-m long plexiglass pipeline. The mixture flows back into the liquid storage tank and is separated by means of a specially designed de-entrainer table. The gas is vented to the atmosphere and the liquid is recirculated into the system.

Flow Visualization System

Figure 3 shows a schematic of the visualization system. The details are shown elsewhere (Gopal and Jepson, 1997). The flow is recorded using two cameras at right angles to the flow. The film height of the liquid before the slug, lengths of

the mixing zone, and total slug lengths were determined from a closeup view, while the slug translational velocity was determined from a second camera placed a sufficient distance away to track the slug over a minimum of ten frames. A ruler was recorded as part of the flow images and this was used to calibrate the resolution of the number pixels in the image and to convert the scale from pixels to centimeters. The video images were then digitized and analyzed on a graphics workstation. All image analysis was performed on video of water-carbon dioxide moving slugs. This was due to the need for high-resolution images that would lend themselves to this type of analysis.

Image Analysis Procedures

Edge tracking was used for image analysis. An algorithm was developed to allow the computer to record the coordinates of any desired point in the image. The point was identified by the movement of a user-controlled cursor which was controlled manually. Several image processing programs were written to

Nomenclature

v_s = translational velocity of slug, m/s
 c_v = conversion factor from pixels to cm
 h = film height, cm

y_b = y-coordinate of pipe bottom, pixels
 x_i = x-coordinate of slug front in image i

n = no. of frames over which slug front is tracked
 y_c = y-coordinate of film surface, pixels

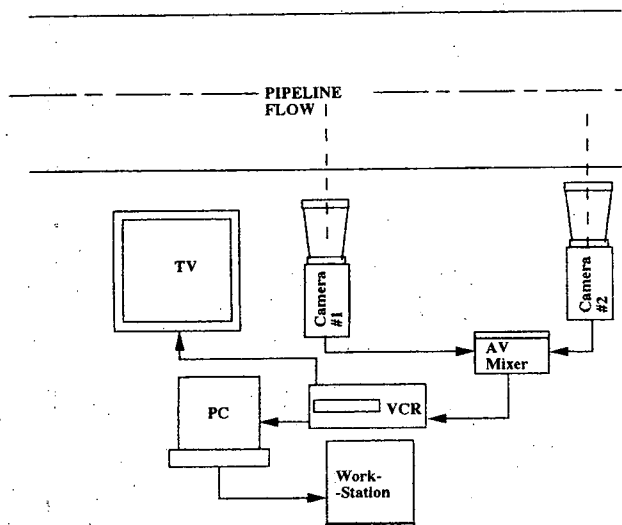


Fig. 3 Schematic diagram of flow visualization system

analyze the images for each type of data, e.g., slug translational velocity, liquid film height, and slug length. Essentially, the image processing scheme involves the creation of a buffer in memory for the display of the image, setting the image size and other relevant parameters, and then drawing the image on the screen. An image analysis subroutine was used to accomplish the necessary edge tracking.

Figure 4 shows a three-dimensional video image of a slug flowing in the pipe. It was found that accurate analysis of this image was extremely difficult due to the extreme turbulence and associated uncertainties in determination of bubble spatial coordinates. Hence a two-dimensional analysis was carried out using the video image at right angles to the flow. Figures 5(a) to (c) show an example of the images used for the analysis. The time-interval between the consecutive images is 0.017 s. This corresponds to the 60 images per s obtained from the video. Using such consecutive images, all the slug characteristics reported in this paper were obtained.

Slug Translational Velocity. Detailed observations of the slug front shows that the leading edge of the slug at the top of the pipe does not move with constant velocity and the shape of the slug front changes significantly in each image. As the slug front scoops up liquid, its leading edge grows rapidly and touches the top of the pipe. This leads to a sudden acceleration of the leading edge. Hence, to obtain an accurate measurement of the slug translational velocity, it is necessary to track the slug front over a sufficient number of frames.



Fig. 4 3-D video image of slug flowing in a pipe

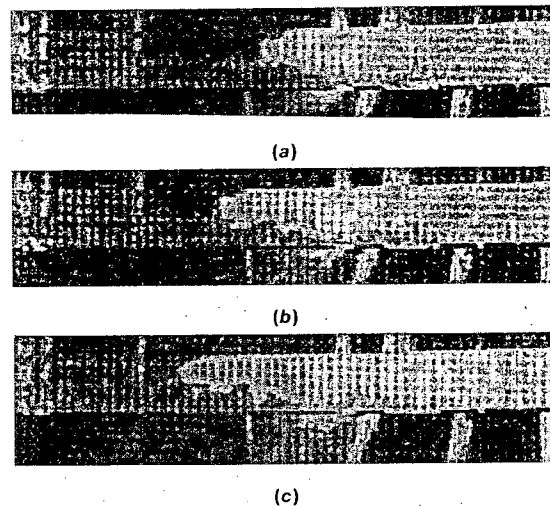


Fig. 5 Consecutive video images of slug—time interval = 0.017 s

This is illustrated by the arrows shown in Figs. 9(a) through (c). The second camera, positioned further back from the flow, was used for this purpose. Typically, the slug front was tracked over 12 to 18 frames. In each image, the coordinates

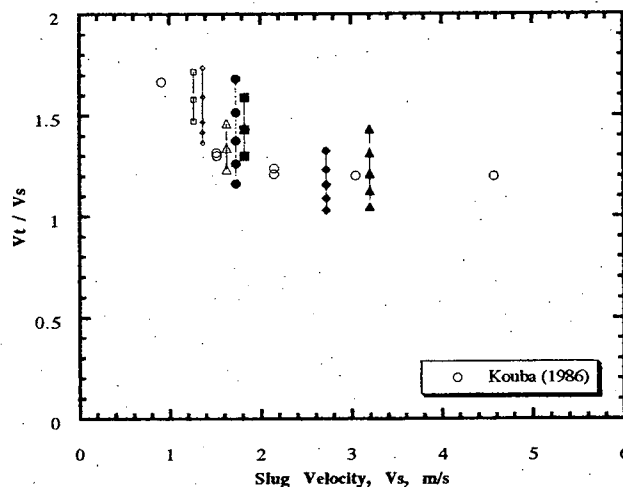


Fig. 6(a) Variation of slug translational velocity with slug velocity water CO_2 system

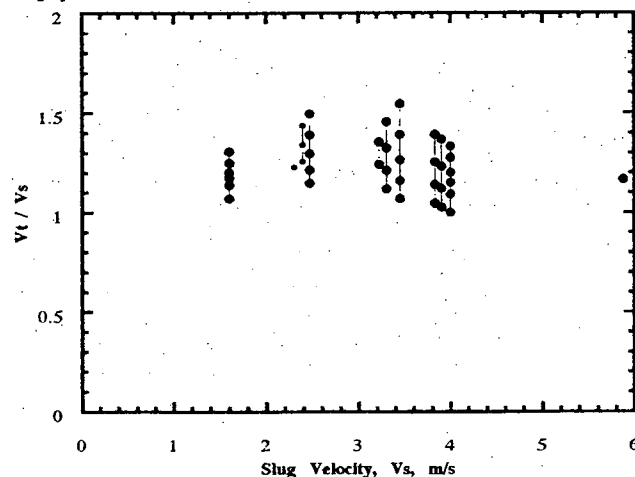


Fig. 6(b) Variation of slug translational velocity with slug velocity ARCOPAK 90™- CO_2 system

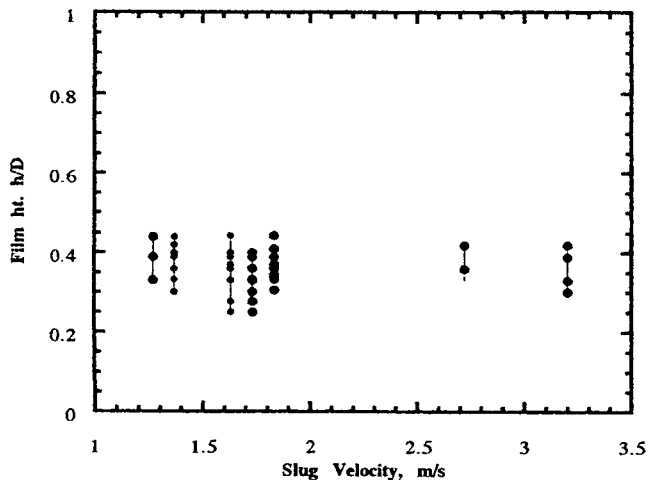


Fig. 7(a) Variation of film height with slug velocity for water-CO₂ system

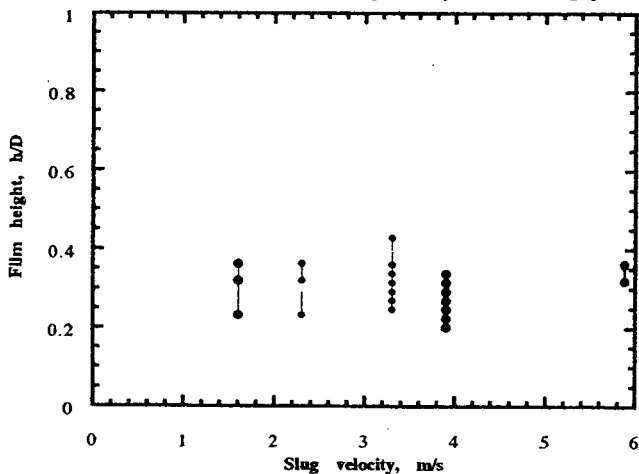


Fig. 7(b) Variation of liquid film height with slug velocity for ARCO-PAC90™-CO₂ system

of the point where the front touches the top of the pipe were recorded.

Once the spatial coordinates of the slug front have been obtained, the slug translational velocity, v_t , may be obtained by the following equation:

$$v_t = \sum_{i=1}^n \frac{x_i - x_{i+1}}{n-1} \frac{1}{c_v \cdot 100} \quad (1)$$



Fig. 8 Video image of mixing zone for $V_{SL} = 0.2$ m/s and $V_{SG} = 1.43$ m/s

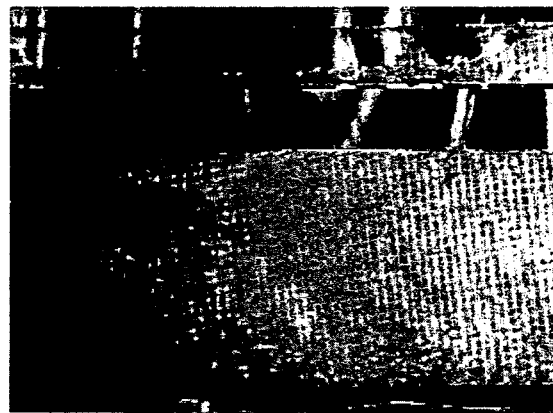


Fig. 9 Video image of mixing zone for $V_{SL} = 0.7$ m/s and $V_{SG} = 2.5$ m/s

Liquid Film Height. The coordinates of the film surface and the bottom of the pipe were recorded with distance, and the film height was calculated. This is given by

$$h = \frac{y_c - y_b}{c_v} \quad (2)$$

Mixing Length. The mixing length is difficult to define. In this study, it is based on two criteria. It was found that beyond a certain distance into the slug, the void fraction distribution in the slug reaches a near-steady-state profile. The minimum distance at which this occurred was defined as the mixing zone. Visually, this also corresponds to the end of the frothy, turbulent, highly aerated part of the slug. It was found that this definition of the mixing length was appropriate to explain the physical mechanisms observed within the slugs. It is shown that the mixing length increases with film Froude number according to the concepts developed in this study. The mixing length was measured as the number of images for which this turbulent part of the slug was in view multiplied by the slug velocity.

Results and Discussion

Slug Translational Velocity. Figures 6(a) and 6(b) show the variation of slug translational velocity, v_t , with slug velocity, v_s . In Fig. 10(a), results presented by Kouba (1986) are also given. It can be seen that the ratio of v_t with v_s decreases with increase in slug velocity. At low slug velocities, the maximum ratio of v_t to v_s is about 1.75, decreasing to about 1.2 at higher slug velocities. These results are similar to those reported by Kouba (1986). Figure 6(b) indicates similar results for ARCO-PAK90™-carbon dioxide slugs.

Liquid Film Height. Figures 7(a) and (b) show the variations of liquid film height ahead of the slug as a function of the slug velocity for water-carbon dioxide (CO₂) and ARCO-PAK90™-CO₂ systems. The liquid film height measurements ahead of the slug vary substantially. The presence of large-amplitude, three-dimensional roll waves on the liquid film between slugs give large spacial variations in the liquid film height. Similar variations are seen for ARCO-PAK90™. The nondimensional average liquid film heights in all cases are between 0.3 and 0.4. This is in agreement with the results shown by Kouba (1986) for a 7.6-cm pipe, and Jepson and Taylor (1988) for a 300-mm-dia pipe, at similar velocities.

Mixing Zone. The mixing zone in the slug is a highly turbulent, frothy region with large amounts of gas entrainment. Figures 7 and 8 show the mixing zone at two different liquid and gas velocities. Figure 7 shows the mixing zone for a superficial liquid velocity of 0.2 m/s and a superficial gas velocity

Table 2 Variation of mixing length as a function of slug velocity for water-carbon dioxide slugs

Slug velocity, m/s	Mixing length, m			
	Minimum	Maximum	Mean	St. Deviation
1.27	0.11	0.32	0.21	0.067
1.37	0.11	0.28	0.18	0.067
1.63	0.27	0.44	0.3	0.058
1.73	0.11	0.41	0.26	0.076
1.83	0.18	0.45	0.28	0.069
2.7	0.23	0.50	0.36	0.069
3.2	0.43	0.85	0.70	0.13

of 1.43 m/s, while Fig. 8 reveals the mixing zone for a superficial liquid and gas velocity of 0.7 and 2.5 m/s, respectively. The film Froude number in Fig. 7 is about 4, while it is about 9 in Fig. 8. It is seen from Figs. 7 and 8 that the length of the mixing zone increases with slug velocity. This is expected since the overall turbulence is increased at the higher velocities. These pulses of bubbles can be seen in Figs. 7 and 8. The length of the mixing zone is determined by the release of pulses of bubbles behind the slug front. The slug front overruns slow moving liquid film ahead of it and assimilates it into the slug creating a mixing vortex behind the slug front. The assimilation of the liquid film accelerates the slug front and it jumps to the top of the pipe, entraining large amounts of gas in the process. This gas is trapped in the mixing vortex and is released into the mixing zone in the form of pulses of bubbles. The mixing of gas and liquid in this region creates large amounts of turbulence resulting in the variation of the length of the mixing zone.

Table 2 shows the distribution of mixing lengths. In this study, the end of the mixing zone was determined by the minimum distance into the slug where the void profile could be described as having reached a quasi-steady state. Visually, this also corresponds to the end of the frothy, highly turbulent region of the slug in the video image.

It is seen from Table 2 that the variation in mixing lengths in all the cases are within ± 1.5 standard deviations. In general, the mixing length increases with an increase in the slug velocity. At a slug velocity of 1.27 m/s, the mixing length is 0.2 m. This increases to about 0.7 m at a slug velocity of 3.2 m/s.

Conclusions

A novel flow visualization system has been developed to study the detailed characteristics of slug flow. Digital image processing algorithms have been developed involving edge-tracking routines to obtain the coordinates of specified points in the image. These coordinate data were used to obtain data on slug translational velocity and liquid film heights.

In the range of velocities studied for the water-carbon dioxide system, the ratio of the slug translational velocity to the slug velocity was found to decrease from 1.75 at a slug velocity of 1.2 m/s to 1.2 above a slug velocity of 2 m/s. The higher ratio at the lower slug velocity was explained by using a drift velocity between gas and liquid. The drift velocity decreases to zero above a slug velocity of 2 m/s. The results agree with those of several other workers (e.g., Kouba, 1986).

The average nondimensional liquid film heights in all cases were between 0.3 and 0.4. Large-amplitude roll waves on the liquid film between slugs were responsible for these film height variations in both systems. This is in agreement with the results of Kouba (1986) and Jepson and Taylor (1988).

Flow visualization was used to develop a new definition for the mixing length in slug flow.

References

- Jepson, W. P., 1987, "The Flow Characteristics in Horizontal Slug Flow," *3rd International Conference on Multiphase Flow*, Paper F2, p. 187.
- Nicholson, M. K., Aziz, K., and Gregory, G. A., 1978, "Intermittent Two Phase Flow in Horizontal Pipes: Predictive Models," *Canadian Journal of Chemical Engineering*, Vol. 56, p. 653.
- Dukler, A. E., and Hubbard, M. G., 1975, "A Model for Gas-Liquid Slug Flow in Horizontal and Near Horizontal Tubes," *Industrial Engineering Chemistry Fundamentals*, Vol. 14, No. 4, pp. 337-347.
- Kouba, G. E., 1984, "Horizontal Slug Flow Modeling and Metering," Ph.D. thesis, University of Tulsa, Tulsa, OK.
- Gopal, M., and Jepson, W. P., 1997, "Development of Digital Image Analysis Techniques for the Study of Velocity and Void Profiles in Slug Flow," *Internal Journal of Multiphase Flow*, Vol. 23, No. 5, pp. 945-965.
- Gopal, M., and Jepson, W. P., 1998, "The Study of Dynamic Slug Flow Characteristics Using Digital Image Analysis—Part II: Modeling Results," *ASME JOURNAL OF ENERGY RESOURCES TECHNOLOGY*, Vol. 120, June, pp. 102-105.
- Gopal, M., Kaul, A., and Jepson, W. P., 1995, "Mechanisms Contributing to Enhanced Corrosion Rates in Three-Phase Slug Flow in Horizontal Pipes," *NACE/95*, Paper 105, pp. 1-16.
- Luo X. K., Jiang, P. J., and Fan, L. S., 1997, "High-Pressure Three-Phase Fluidization: Hydrodynamics and Heat Transfer," *AIChE Journal*, Vol. 43, No. 10, pp. 2432-2445.
- Jepson, W. P., and Taylor, R. E., 1988, "Slug Flow and its Transitions in Large Diameter Horizontal Pipes," *AERE-R12992*, Harwell Laboratories, U.K.
- Miles, R. B., and Lempert, W. R., 1997, "Quantitative Flow Visualization in Unseeded Flows," *Annual Review of Fluid Mechanics*, Vol. 29, pp. 285-326.